

Antiferromagnetic Spin Fluctuations and Unconventional Nodeless Superconductivity in an Iron-based New Superconductor $(\text{Ca}_4\text{Al}_2\text{O}_{6-y})(\text{Fe}_2\text{As}_2)$: ^{75}As -NQR Study

H. Kinouchi,^{1,*} H. Mukuda,^{1,2,†} M. Yashima,^{1,2} Y. Kitaoka,¹ P. M. Shirage,^{3,2} H. Eisaki,^{3,2} and A. Iyo^{3,2}

¹Graduate School of Engineering Science, Osaka University, Osaka 560-8531, Japan

²JST, TRIP (Transformative Research-Project on Iron Pnictides), Chiyoda, Tokyo 102-0075, Japan

³National Institute of Advanced Industrial Science and Technology (AIST), Umezono, Tsukuba 305-8568, Japan

(Dated: July 23, 2018)

We report ^{75}As -nuclear quadrupole resonance (NQR) studies on $(\text{Ca}_4\text{Al}_2\text{O}_{6-y})(\text{Fe}_2\text{As}_2)$ with $T_c = 27$ K, which unravel unique normal-state properties and point to unconventional nodeless superconductivity (SC). Measurement of nuclear-spin-relaxation rate $1/T_1$ has revealed a significant development of two dimensional (2D) antiferromagnetic (AFM) spin fluctuations down to T_c , in association with the fact that FeAs layers with the smallest As-Fe-As bond angle are well separated by thick perovskite-type blocking layer. Below T_c , the temperature dependence of $1/T_1$ without any trace of the coherence peak is well accounted for by an s_{\pm} -wave multiple gaps model. From the fact that $T_c = 27$ K in this compound is comparable to $T_c=28$ K in the optimally-doped LaFeAsO_{1-y} in which AFM spin fluctuations are not dominant, we remark that AFM spin fluctuations are not a unique factor for enhancing T_c among existing Fe-based superconductors, but a condition for optimizing SC should be addressed from the lattice structure point of view.

Iron-based high- T_c superconductors[1] comprise a two-dimensional layered structure of iron (Fe)-pnictgen (Pn) planes, which are separated by blocking layers, such as LnO (Ln =rare earth), alkaline earth, and alkaline metal elements. Relatively high SC transition has been reported in Fe-pnictides with a thick perovskite-type blocking layer, in which the interlayer distance between $FePn$ layers is more than ~ 13 Å [2–5]. For example, T_c is ~ 47 K for $(\text{Ca}_4(\text{Mg}_{0.25}\text{Ti}_{0.75})_3\text{O}_y)(\text{Fe}_2\text{As}_2)$ [4], and ~ 37 K for $(\text{Sr}_4\text{V}_2\text{O}_6)(\text{Fe}_2\text{As}_2)$ [2], which rises up to 46 K by the application of pressure[6]. Moreover, in these series of Fe-based compounds, neither structural transition nor magnetic order has been reported so far, differentiating them from other Fe-based superconductors that emerge in close proximity to antiferromagnetic (AFM) order[1]. In fact, the maximum of SC transition temperature T_c seems to take place around a quantum-critical point (QCP) of AFM order for $\text{Ba}(\text{Fe}_{1-x}\text{Co}_x)_2\text{As}_2$ [7] and $\text{BaFe}_2(\text{As}_{1-x}\text{P}_x)_2$ [8, 9]. On the one hand, the T_c of Fe-pnictides is intimately related with local structural parameters such as a Pn -Fe- Pn bond angle of $FePn_4$ tetrahedron (*Lee's plot*)[10] and/or a height of pnictgen from $FePn$ -plane[11]. In this context, systematic investigations on Fe-based superconductors with a thick blocking layer are required in order to get insight into some correlation between T_c and structural parameters and/or AFM spin fluctuations.

In this Letter, we report ^{75}As -nuclear quadrupole resonance (NQR) studies on $(\text{Ca}_4\text{Al}_2\text{O}_{6-y})(\text{Fe}_2\text{As}_2)$ with $T_c = 27$ K that unravel the development of significant AFM spin fluctuations and point to unconventional nodeless superconductivity (SC).

A polycrystalline sample of $(\text{Ca}_4\text{Al}_2\text{O}_{6-y})(\text{Fe}_2\text{As}_2)$ with a nominal content of $y \sim 0.215$ (denoted as Al-42622 hereafter) was synthesized by solid-state reaction method using high-pressure synthesis technique as de-

scribed elsewhere[5]. Powder x-ray diffraction measurement indicates that this sample is almost composed of a single phase with lattice parameters, $a=3.71$ Å and $c=15.40$ Å. This compound is characterized by a small a -axis length, a narrow Pn -Fe- Pn bond angle ($\alpha \sim 102.1^\circ$), and a high Pn distance from $FePn$ plane with $h_{Pn} \sim 1.50$ Å[5]. $T_c = 27$ K was determined from the onset of SC diamagnetism in susceptibility measurement. ^{75}As -NQR measurements have been performed on a coarse powder sample at zero external field.

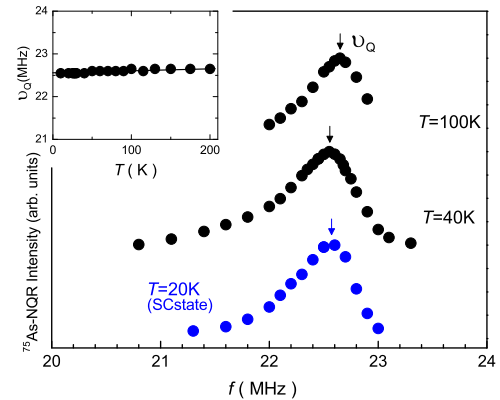


FIG. 1: (Color online) ^{75}As -NQR spectra of Al-42622. The inset shows T dependence of $^{75}\nu_Q$ of Al-42622, indicating that neither structural phase transition nor no magnetic order takes place in Al-42622.

Figure 1(a) shows ^{75}As -NQR spectra of Al-42622. ^{75}As -NQR frequency ($^{75}\nu_Q$) is ~ 22.6 MHz, which is the largest among Fe-based superconductors so far. In $Ln\text{FeAsO}_\delta$ (Ln :Rare earth, denoted as Ln -1111 hereafter), note that $^{75}\nu_Q$ becomes large when an a -axis length decreases[12, 13]. Since $^{75}\nu_Q$ is proportional to an electric field gradient at ^{75}As nuclear site yielded by

local distributions of on-site electron density and lattice ions around an ^{75}As nucleus. In this context, the fact that $^{75}\nu_Q$ in Al-42622 is the largest among other Fe-based compounds may be because its a -axis length is the shortest. The ^{75}As -NQR spectrum is almost temperature (T) independent in a range of 10 K and 200 K, as shown in the inset of Fig. 1, demonstrating that neither structural phase transition nor magnetic order takes place in Al-42622. An asymmetric shape of the ^{75}As -NQR spectra in Al-42622 is probably caused by some distribution of oxygen deficiency y .

^{75}As -NQR $1/T_1$ is obtained by fitting a recovery curve of ^{75}As nuclear magnetization to a single exponential function $m(t) \equiv (M_0 - M(t))/M_0 = \exp(-3t/T_1)$ for $I=3/2$. Here M_0 and $M(t)$ are the respective nuclear magnetizations for a thermal equilibrium condition and at time t after a saturation pulse. In Al-42622, $m(t)$ was reproduced by a single component of $1/T_1$ above 40 K, but not below ~ 40 K, as shown in Figs. 2(a) and 2(b), respectively. Since the short component $1/T_{1S}$ and the long one $1/T_{1L}$ below ~ 40 K exhibit almost the same T dependence when normalized at T_c (see Fig. 3(a)), we focus on the T dependence of $1/T_{1S}$ which is a dominant component below 40 K.

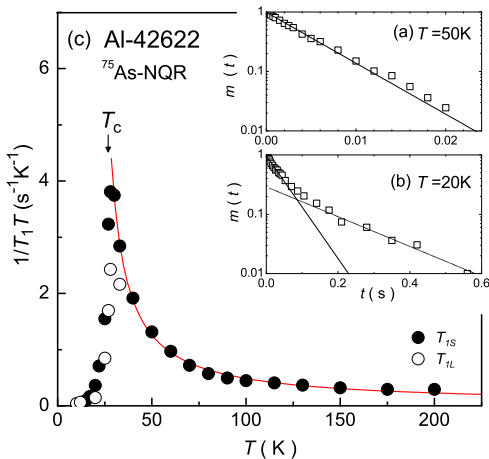


FIG. 2: (Color online) Recovery curves of ^{75}As nuclear magnetization $m(t)$ at (a) 50 K and (b) 20 K. (c) T dependence of $1/T_1T$ for Al-42622. The solid curve is a simulation fitted to a relation $1/T_1T \sim a/(T + \theta) + b$ with parameters $a=37$, $\theta=-20$ K, and $b=0.023$.

Figure 2(c) shows the T dependence of ^{75}As -NQR $1/T_1T$ for Al-42622. The $1/T_1T$ in the normal state increases significantly upon cooling down to T_c . The AFM spin fluctuations in Fe-based superconductors are enhanced by the nesting of hole and electron Fermi surfaces (FSs). In general, $1/T_1T$ is described as $1/T_1T \propto \sum_{\mathbf{q}} |A_{\mathbf{q}}|^2 \chi''(\mathbf{q}, \omega_0)/\omega_0$, where $A_{\mathbf{q}}$ is a wave-vector (\mathbf{q})-dependent hyperfine-coupling constant, $\chi(\mathbf{q}, \omega)$ a dynamical spin susceptibility, and ω_0 an NQR frequency. When a system is close to an AFM QCP, two-dimensional

(2D) AFM spin-fluctuation model predicts a relation of $1/T_1T \propto \chi_Q(T) \propto 1/(T + \theta)$ [14]. Here, staggered susceptibility $\chi_Q(T)$ with an AFM propagation vector $\mathbf{q}=\mathbf{Q}$ follows a Curie-Weiss law. Since $1/T_1T$ diverges towards $T \rightarrow 0$ when $\theta = 0$, θ is a measure of how close a system is to an AFM QCP. Actually, as shown by the solid line in Fig. 2(c), the $1/T_{1S}T$ in Al-42622 can be fitted by assuming $1/T_1T \sim a/(T + \theta) + b$ with parameters $a=37$, $\theta=-20$ K, and $b=0.023$. It is unexpected that θ is negative, meaning that the staggered susceptibility would diverge toward 20K, and hence an AFM order would be anticipated below ~ 20 K. As a matter of fact, in the case of $\text{Ba}(\text{Fe}_{1-x}\text{Co}_x)_2\text{As}_2$ and $\text{BaFe}_2(\text{As}_{1-x}\text{P}_x)_2$, the AFM order sets in when θ becomes negative [7, 9]. However, SC occurs below $T_c=27$ K in Al-42622, instead of an AFM order. This is because a thick blocking layer between FeAs layers makes an interlayer magnetic coupling weak, suppressing an onset of AFM order. Besides, the structure consisting of perovskite blocks bonded by strong covalent bonding prevents a structural phase transition into an orthorhombic phase. These might be the main reasons why an AFM order of FePn layers is absent in the Fe-pnictides family with the thick blocking layers.

The band calculation for Al-42622 reported by Miyake *et al.* revealed that a hole FS around Γ' (π, π) in the unfolded FS regime appears explicitly as a result of the small $\alpha \sim 102^\circ$, whereas one of two-hole FSs at $\Gamma(0,0)$ is missing [15]. Eventually, it is concluded that the well nested FS topology between hole FSs at Γ and Γ' , and electron FSs at $M((0, \pi)$ and $(\pi, 0)$) enhances a Stoner factor of antiferromagnetism in Al-42622 [16]. This event leads to the development of AFM spin fluctuations and hence is consistent with the experiment presented here.

Next, we address SC characteristics emerging under the background of AFM spin fluctuations. Figure 3(a) shows a plot of $T_1(T_c)/T_1$ normalized at T_c against T/T_c , exhibiting a steep decrease upon cooling without the coherence peak just below T_c . The T dependence of $1/T_1$ seems to follow a $\sim T^7$ dependence down to $\sim 0.3T_c$, which is quite unique as compared with the T^3 in optimally-doped La-1111(OPT) with $T_c=28$ K [12, 17] and the T^5 in optimally-doped $\text{Ba}_{0.6}\text{K}_{0.4}\text{Fe}_2\text{As}_2$ (BaK122(OPT)) with $T_c=38$ K [18]. Notably, Fig. 3(b) shows the T dependence of $1/T_1T$ normalized at $T=250$ K in these compounds. We remark that as AFM spin fluctuations are more significantly enhanced, a power-law reduction in $1/T_1$ below T_c becomes steeper from $\sim T^3$ to $\sim T^7$.

In previous studies [18, 19], the non-universal T -dependence in $1/T_1$ was consistently accounted for by a multigap nodeless s_{\pm} -wave pairing model [21–25]. In the s_{\pm} -wave model with two isotropic gaps, an initial decrease of $1/T_1$ without the coherence peak just below T_c is due to the opening of a large SC gap with $2\Delta_0^L/k_B T_c$ [19]. As seen in Fig. 4(a), the initial decrease in $1/T_1$ just below T_c in Al-42622 is similar to that in

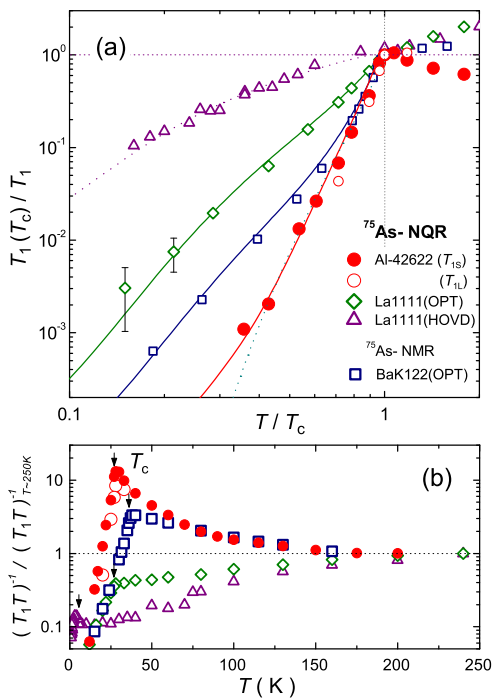


FIG. 3: (Color online) (a) Plots of $^{75}\text{As-NQR}$ $T_1(T_c)/T_1$ normalized at T_c against T/T_c for Al-42622, along with the results of BaK122(OPT) with $T_c=38$ K [18], La1111(OPT) with $T_c=28$ K [12], and La1111(HOVD) with $T_c=5$ K [20]. Note that T dependences of T_{1S} and T_{1L} normalized at T_c for Al-42622 are almost the same below T_c . The solid curves are simulations in terms of the s_{\pm} -wave model with multiple SC gaps (see text). (b) T dependence of $^{75}\text{As-NQR}$ $(1/T_1T)^{1/7}$ normalized at $T=250$ K.

BaK122(OPT). This means that the large SC gap is comparable in these compounds. On the other hand, the $1/T_1$ for Al-42622 decreases more steeply than in BaK122(OPT) as temperature falls well below T_c . This is primarily because the fraction of the density of states (DOS) at the Fermi level for FSs with a small SC gap, $r_S \equiv N_S^S/(N_S^L + N_S^S)$ is smaller for Al-42622 than for BaK122(OPT). Here N_L and N_S represent the respective DOSs with large and small SC gaps. Actually, the result was well reproduced, assuming that $r_S \sim 0.1$ for Al-42622 is smaller than $r_S \sim 0.3$ for BaK122(OPT) [18]. It is deduced that N_S^S is significantly smaller in Al-42622 than in BaK122(OPT). Note that in the simulation, a gap ratio $\Delta_0^S/\Delta_0^L=0.35$, a smearing factor $\eta=0.14\Delta_0^L$, and a coefficient of coherence factor $\alpha_c \sim 0$ (see Ref.[20]) were used in BaK122(OPT) [18] for simplicity. Even when $N_S^S=0$ or $r_S=0$ is assumed, the experiment can be also reproduced with $\eta \sim 0.3\Delta_0^L$ larger than $\eta=0.14\Delta_0^L$ for $r_S \sim 0.1$, as shown by the broken line in Fig. 4(a).

Next, we present an attempt to simulate a relaxation behavior below T_c for various Fe-based superconductors by changing the coefficient of coherence factor α_c . In this simulation, $\alpha_c = 1$ is assumed for sign-conserving

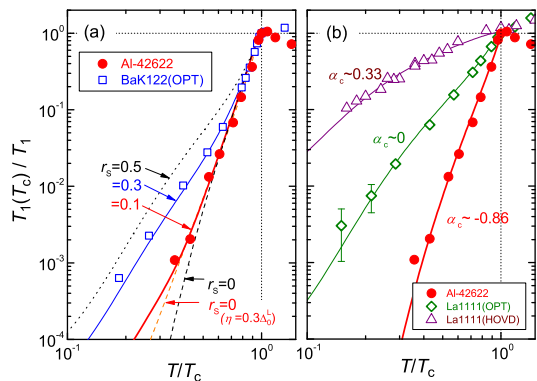


FIG. 4: (Color online) (a) Plots of $^{75}\text{As-NQR}$ $T_1(T_c)/T_1$ normalized at T_c against T/T_c for Al-42622 and BaK122(OPT) with $T_c=38$ K [18]. The curves are simulations in terms of the s_{\pm} -wave model with two isotropic gaps with various values of $r_S \equiv N_S^S/(N_S^L + N_S^S)$. Here N_L and N_S represent the respective DOSs with large and small SC gaps. The experimental result for Al-42622 was reproduced with $r_S \sim 0.1$, which is smaller than $r_S \sim 0.3$ for BaK122(OPT) [18]. (b) Similar plots for Al-42622, La1111(OPT) with $T_c=28$ K [12] and La1111(HOVD) with $T_c=5$ K [20]. The experiment for Al-42622 can be also reproduced by assuming a *negative* value of $\alpha_c \sim -0.86$, which contrasts with $\alpha_c \sim 0.33$ in La1111(HOVD) and $\alpha_c \sim 0$ in La1111(OPT).

*intra*band scattering and $\alpha_c = -1$ for sign-nonconserving *inter*band scattering. The value varies in the range $-1 \leq \alpha_c \leq 1$ dependent on the weight of their contribution in the nuclear relaxation process. In the previous studies on the heavily-overdoped $\text{LaFeAsO}_{1-x}\text{F}_x$ (La1111(HOVD)) with $T_c=5$ K [20] and optimally-doped La1111 (OPT) with $T_c=28$ K [12], the experiments were reproduced with $\alpha_c \sim 0.33$ for La1111(HOVD) and $\alpha_c \sim 0$ for La1111(OPT), as shown in Fig. 4(b), which is attributed to the fact that the nesting condition of FSs becomes significantly worse in heavily overdoped regime. On the other hands, in Al-42622, AFM spin fluctuations develop significantly due to more dominant interband scattering than in the others. Relevant to this event, the experiment can be also reproduced by assuming a *negative* value of $\alpha_c \sim -0.86$, as indicated in Fig. 4(b), which contrasts with the previous studies. Here, $r_S \leq 0.1$ and $2\Delta/k_B T_c=6.1$ were used along with other parameters used in La1111(OPT) with $T_c=28$ K [18, 20]. It should be noted that the overall T dependence of $1/T_1$ below T_c in Fe-based superconductors is consistently accounted for by the s_{\pm} -wave model with isotropic multiple gaps mainly through changing the coefficient of coherence factor α_c . We highlight the fact that the dominant *inter*band scattering due to the nesting of hole and electron FSs is responsible for the marked enhancement of 2D AFM spin fluctuations and the sign-nonconserving *inter*band scattering is responsible for the T^7 -like reduction behavior in $1/T_1$ without the coherence peak below T_c .

We have shown two possible simulations to reproduce

the characteristic T dependence of $1/T_1$ in the SC state of Al-42622. It is notable that, in either case, the assumption of $r_S \leq 0.1$ and $\alpha_c \leq 0$ were necessary, implying that the SC gaps on hole and electron FSs are nodeless with comparable sizes and the opposite signs. This event may be related to the band-calculation result that one of the hole FSs around $\Gamma(0,0)$ disappears[15]. Nevertheless, AFM spin fluctuations are more significant in Al-42622 with $T_c=27$ K than in La1111(OPT) with $T_c=28$ K, but T_c is comparable for both. This result reveals that AFM spin fluctuations are not a unique factor for enhancing T_c . Theoretically, within a spin-fluctuation mediated pairing theory on a five-orbital model, Usui *et al.* have claimed that the reduction of multiplicity of FSs in Al-42622 is a main reason why the T_c of Al-42622 is not so high even when AFM spin fluctuations are more remarkable than in existing Fe-based superconductors[16]. Since the FS topology is tuned by varying structural parameters such as pnictogen height and As-Fe-As bond angle α , further systematic experiments are desired on a same series of Fe-based compounds.

Finally, we comment on an s_{++} -wave model within orbital-fluctuation mediated pairing theory[26]. In general, the suppression of the coherence peak takes place in the strong-coupling regime of s -wave SC with relatively high T_c since strong-coupling effect causes T_c not only to increase, but also causes the lifetime of quasiparticles to shorten due to some damping effect[27, 28]. For example, in a strong-coupling s -wave superconductor $\text{TiMo}_6\text{Se}_{7.5}$ with $T_c=12.2$ K, the coherence peak is suppressed due to the phonon damping effect more significantly than in a weak-coupling one $\text{Sn}_{1.1}\text{Mo}_6\text{Se}_{7.5}$ with $T_c=4.2$ K[27]. A similar behavior was also observed for MgB_2 ($T_c \sim 40$ K) and NbB_2 ($T_c=5$ K)[28]. In Fe-based superconductors, the marked decrease of $1/T_1$ just below T_c is most significant in Al-42622 with $T_c=27$ K among existing Fe-based superconductors, despite the fact that T_c is not so high relatively. It seems unlikely that the suppression of the coherence peak observed universally in most Fe-based superconductors can be systematically accounted for in terms of an s_{++} -wave model. Moreover, a non-magnetic impurity effect in La1111 compounds is not compatible with the s_{++} -wave state at all; While the crystal structure and electronic state are not modified by non-magnetic Zn substitution, the SC with $T_c = 24$ K disappears by 3% Zn substitution [29, 30].

In conclusion, the ^{75}As -NQR studies on $(\text{Ca}_4\text{Al}_2\text{O}_{6-y})(\text{Fe}_2\text{As}_2)$ with $T_c = 27$ K have unraveled the development of 2D AFM spin fluctuations and pointed to the unconventional nodeless SC; The dominant interband scattering due to the nesting of hole and electron FSs is responsible for the marked enhancement of 2D AFM spin fluctuations and the sign-nonconserving interband scattering is responsible for the T^7 -like reduction behavior in $1/T_1$ without the coherence peak below T_c . The T evolution in $1/T_1$ in the

SC state was consistently accounted for by the s_{\pm} -wave multiple gaps model. The present result also suggests that the DOS with a small SC gap is totally reduced in association with the disappearance of some part of Fermi surfaces. From the fact that $T_c = 27$ K in this compound is comparable to $T_c=28$ K in the optimally-doped LaFeAsO_{1-y} in which AFM spin fluctuations are not dominant, we remark that AFM spin fluctuations are not a unique factor for enhancing T_c , but a condition for optimizing SC should be addressed from the lattice structure point of view.

We thank K. Kuroki for valuable comments. This work was supported by a Grant-in-Aid for Specially Promoted Research (20001004) and by the Global COE Program (Core Research and Engineering of Advanced Materials-Interdisciplinary Education Center for Materials Science) from the Ministry of Education, Culture, Sports, Science and Technology (MEXT), Japan.

* e-mail address: kinouchi@nmr.mp.es.osaka-u.ac.jp

† e-mail address: mukuda@mp.es.osaka-u.ac.jp

- [1] Y. Kamihara *et al.*, J. Am. Chem. Soc. **130**, 3296 (2008).
- [2] X. Zhu *et al.*, Phys. Rev. B **79**, 220512(R) (2009).
- [3] H. Ogino *et al.*, Supercond. Sci. Technol. **22**, 085001 (2009).
- [4] H. Ogino *et al.*, Appl. Phys. Expr. **3** 063103 (2010).
- [5] P. M. Shirage *et al.*, Appl. Phys. Lett. **97**, 172506 (2010).
- [6] H. Kotegawa *et al.*, J. Phys. Soc. Jpn. **78**, 123707 (2009).
- [7] F. L. Ning *et al.*, Phys. Rev. Lett. **104**, 037001 (2010).
- [8] S. Kasahara *et al.*, Phys. Rev. B **81**, 184519 (2010).
- [9] Y. Nakai *et al.*, Phys. Rev. Lett. **105**, 107003 (2010).
- [10] C. H. Lee *et al.*, J. Phys. Soc. Jpn. **77**, 083704 (2008).
- [11] Y. Mizuguchi *et al.*, Supercond. Sci. Technol. **23**, 054013 (2010).
- [12] H. Mukuda *et al.*, J. Phys. Soc. Jpn. **77**, 093704 (2008).
- [13] H. Mukuda *et al.*, Physica C **469**, 559 (2009).
- [14] T. Moriya and K. Ueda, Adv. Phys. **49**, 555 (2000).
- [15] T. Miyake *et al.*, J. Phys. Soc. Jpn. **79**, 123713 (2010).
- [16] H. Usui and K. Kuroki, Phys. Rev. B, *in press* (arXiv 1102.3765).
- [17] Y. Nakai *et al.*, J. Phys. Soc. Jpn. **77**, 073701 (2008).
- [18] M. Yashima *et al.*, J. Phys. Soc. Jpn. **78**, 103702 (2009).
- [19] H. Yamashita *et al.*, J. Phys. Soc. Jpn. **79**, 103703 (2010).
- [20] H. Mukuda *et al.*, J. Phys. Soc. Jpn. **79**, 113701 (2010).
- [21] D. Parker *et al.*, Phys. Rev. B **78**, 134524 (2008).
- [22] A. V. Chubukov, D. V. Efremov, and I. Eremin, Phys. Rev. B **78**, 134512 (2008).
- [23] Y. Bang and H. Y. Choi, Phys. Rev. B **78**, 134523 (2008).
- [24] M. M. Parish, J. Hu, and B. A. Bernevig, Phys. Rev. B **78**, 144514 (2008).
- [25] Y. Nagai *et al.*, New J. Phys. **10**, 103026 (2008).
- [26] H. Kontani and S. Onari, Phys. Rev. Lett. **104**, 157001 (2010).
- [27] S. Ohsugi *et al.*, J. Phys. Soc. Jpn. **61**, 3054 (1992).
- [28] H. Kotegawa *et al.*, Phys. Rev. B **66**, 064516 (2002).
- [29] Y. F. Guo *et al.*, Phys. Rev. B **82**, 054506 (2010).
- [30] S. Kitagawa *et al.*, Phys. Rev. B **83**, 180501 (2011).